

Suárez, G. ; Santschi, C. ; Plateel, G. ; Martin, O.J.F. ; Riediker, M. **Absorbance enhancement in microplate wells for improved-sensitivity biosensors.** Biosensors and Bioelectronics, 56:198-203, 2014.

Postprint version	Final draft post-refereeing
Journal website	<a href="http://www.sciencedirect.com/science/journal/09565663">http://www.sciencedirect.com/science/journal/09565663</a>
Pubmed link	<a href="http://www.ncbi.nlm.nih.gov/pubmed/24491962">http://www.ncbi.nlm.nih.gov/pubmed/24491962</a>
DOI	<a href="https://doi.org/10.1016/j.bios.2013.12.063">10.1016/j.bios.2013.12.063</a>

# Absorbance enhancement in microplate wells for improved-sensitivity biosensors

*Guillaume Suárez,<sup>†\*</sup> Christian Santschi,<sup>‡</sup> Gregory Plateel,<sup>†</sup> Olivier J. F. Martin<sup>‡</sup> and Michael Riediker<sup>†</sup>*

<sup>†</sup>Institute for Work and Health, Route de la Corniche 2, CH-1066 Epalinges-Lausanne, Switzerland

<sup>‡</sup>Nanophotonics and Metrology Laboratory, Swiss Federal Institute of Technology Lausanne (EPFL), EPFL-STI-NAM, Station 11, CH-1015 Lausanne, Switzerland.

## RECEIVED DATE

\*Corresponding Author: [guillaume.suarez@epfl.ch](mailto:guillaume.suarez@epfl.ch); Tel: +41 21 314 58 97; Fax: +41 21 314 74

21

KEYWORDS: absorbance enhancement • optical biosensor • hydrogen peroxide • random medium • multiwell microplate

## ABSTRACT

A generic optical biosensing strategy was developed that relies on the absorbance enhancement phenomenon occurring in a multiple scattering matrix. Experimentally, inserts made of glass fiber membrane were placed into microplate wells in order to significantly lengthen the trajectory of the incident light through the sample and therefore increase the corresponding absorbance. An

enhancement factor was calculated by comparing the absorbance values measured for a given amount of dye with and without the absorbance-enhancing inserts in the wells. Moreover, the dilution of dye in solutions with different refractive indices (*RI*) clearly revealed that the enhancement factor increases with the  $\Delta RI$  between the membrane and the surrounding medium, reaching a maximum value ( $EF > 25$ ) when the membranes were dried. On this basis, two  $H_2O_2$ -biosensing systems were developed based on the biofunctionalization of the glass fiber inserts either with cytochrome *c* or horseradish peroxidase (HRP) and the analytical performances were systematically compared with the corresponding bioassay in solution. The efficiency of the absorbance-enhancement approach was particularly clear in the case of the cytochrome *c*-based biosensor with a sensitivity gain of 40-folds and wider dynamic range. Therefore, the developed strategy represents a promising way to convert standard colorimetric bioassays into optical biosensors with improved sensitivity.

## 1. INTRODUCTION

Colorimetric detection technologies provide to the analyst a valuable set of tools suitable to perform routine tests for biomedical diagnosis or environmental monitoring purposes. Despite their diversity in terms of format – ranging from standard cuvettes (Kuang et al. 2007) to multiwell microplates, (Gillespie and Ainsworth 2007) optical fibers (Malcik et al. 2005) or dipsticks (Liu et al. 2006) – the detection principle indistinctively bares on measuring changes in absorbance, as being the physical response to a specific chemical reaction or biological recognition event. The most popular representative of colorimetric tests is the so-called enzyme-linked immunosorbent assay, referred as ELISA, which combines high throughput and high sensitivity for quantitative or semi-quantitative detection of a large number of analytes (Martinez 2011; Plested et al. 2003). Here, the measured absorbance change relies on the enzymatic

conversion of a substrate into a chromogenic compound. Recently, the integration of novel materials in colorimetric detection systems has enlarged their capabilities thanks to their conformation-dependent absorption properties or pseudo-enzymatic catalytic behavior (Song et al. 2011). Typically, for a given system the absorbance change consecutive to the assembly (or disassembly) of functionalized gold nanoparticles (NPs) in a colloidal solution provides a sensitive indication on the presence of chemical (e.g. metal ions (Liu and Lu 2003) or pH (Chen et al. 2008)) or biological (e.g. ssDNA (Mao et al. 2009; Sato et al. 2003), adenosine (Liu et al. 2006)) factors that control this mechanism. On the other side, some metal oxide NPs such as iron oxide (Fe<sub>3</sub>O<sub>4</sub>) have shown to exhibit an intrinsic mimetic peroxidase activity (Gao et al. 2007) which enabled their use as detection labels in ELISA or in H<sub>2</sub>O<sub>2</sub>-based melamine sensors (Ding et al. 2010). In order to improve the analytical performances of colorimetric detection systems the main effort has focused at the reaction/recognition level by seeking catalysts with higher reaction rates and recognition biomolecules with higher affinity constants. However, another track for sensitivity-enhancement strategies is clearly indicated by the physical nature of absorbance, governed by Beer-Lambert law:

$$A = \epsilon.l.C \quad (1)$$

Being the molar absorptivity,  $\epsilon$ , inherent to the species which is found at the molar concentration  $C$  in the sample, and while the path length of light,  $l$ , remains an adaptable parameter.

Therefore, an interesting perspective to develop colorimetric assays with improved sensitivity resides in the ability to lengthen the trajectory of light through the sample. Such an approach is manifest in the detection systems based on either long path flow cell where the light is guided through a few meters long capillary filled with the assay mixture (Zhang 2006) or on-chip lateral beam guidance device particularly suitable for low-aspect-ratio sensing chambers (Grumann et al.

2006). However, in these strategies the gain in sensitivity is due to the fact that a larger volume of the sample – that is a higher number of absorbing molecules – is getting probed by the light. In other words, in such approaches the intrinsic sensitivity understood as the amplitude of signal generated per mole of absorber remains theoretically unchanged. In contrast, we have recently reported that the absorption spectrum of a given biomolecule loaded into a random medium, such as cytochrome *c* embedded into an aggregate of polystyrene beads, results enhanced due to the elongation of the light optical path (Suárez et al. 2012; Suárez et al. 2013). In those preliminary studies the cytochrome *c* absorbance enhancement was efficiently used to develop a sensitive photonic biosensor able to detect in real-time the release of H<sub>2</sub>O<sub>2</sub> by cells under oxidative stress. In the present work, we further extend the biodetection approach to the use of protein-functionalized glass fiber membranes as absorbance enhancing inserts adapted to microplate wells and which exhibit improved sensitivity compared to their corresponding bioassays in solution. In addition, this study experimentally proves the dependency of such an absorbance enhancement on the refractive index difference,  $\Delta RI$ , between the scattering matrix and the surrounding medium.

## 2. MATERIALS AND METHODS

### 2.1 Chemicals

Horseradish peroxidase (HRP type VI, 250-320 U.mg<sub>solid</sub><sup>-1</sup>), cytochrome *c* from bovine heart ( $\geq 95\%$ ), glutaraldehyde solution 25%, hydrogen peroxide (30%), 3-amino-9-ethylcarbazole (AEC), bromocresol green sodium salt (BCG), ethanol, sodium ascorbate, phosphate disodic, phosphate monosodic, sodium chloride, calcium chloride and sodium acetate were all purchased from Sigma-Aldrich (Buchs; Switzerland).

### 2.2 Materials

Clear polystyrene flat bottom 96-wells microplates were provided by Corning (Corning Inc., NY, USA). For the insert-based biosensor approach a circular aperture was drilled at the bottom of the wells bottom using a 2 mm diameter drill bit. Absorbance-enhancer inserts were cut out from glass fiber membranes GF/B (1 mm thickness) purchased from Membrane Solutions (North Bend, USA).

### *2.3 Glass fiber membrane loaded with BCG*

In the experiments involving BCG, clean membrane inserts are placed in standard microplate wells before loading with 25  $\mu\text{L}$  of BCG solution (120  $\mu\text{M}$ ) containing different amount of glucose from 0 to 80%.

### *2.4 Biofunctionalization glass fiber membranes*

Enhancer inserts made from glass fiber membrane are place in the wells of the modified microplate (with bottom aperture) and are subsequently biofunctionalized with either cytochrome *c* or HRP via the following protocol: 25  $\mu\text{L}$  of the protein solution (1  $\text{mg}\cdot\text{mL}^{-1}$  HRP or 25  $\mu\text{M}$  of cytochrome *c*) containing 0.5% of glutaraldehyde is added immediately after preparation onto each clean membrane insert and left to react for 30 min at room temperature. Then, the protein-modified membrane inserts are rinsed intensively by flowing several times PBS pH 7.2 or acetate buffer pH 5.0, for cytochrome *c* and HRP, respectively. In the case of cytochrome *c*-based biosensor, the heme-group was getting reduced prior to measurements by flowing several times 100  $\mu\text{L}$  of ascorbic acid (1 mM in PBS) through the modified membrane. The cytochrome *c*-membranes are finally rinsed intensively with PBS solution.

### *2.4 Absorbance measurements*

All the absorbance measurements are performed on a Infinite® 200 PRO multimode microplate reader from Tecan Group Ltd. The optimal reading wavelengths for BCG, HRP/AEC and cytochrome *c* are 621, 580 and 542/550/556 nm, respectively.

### 3. RESULTS AND DISCUSSION

As depicted in Figure 1 the signal amplification principle relies on physical properties of the light propagating into strongly scattering materials (Svensson and Shen 2010). In the classic bioassay configuration light travels in straight line through the absorber-containing solution and the resulting absorbance, at a given wavelength, varies linearly with both the path length of the sample and the concentration of the absorber, as stated by Beer-Lambert law (eq.1). In contrast, the propagation of light into a non-uniform material is controlled by a multiple scattering regime and its path length then largely exceeds the geometrical dimension of the sample (John and Pang 1996; Popescu and Dogariu 1999). Consequently to the path length amplification due to light diffusion in strongly scattering medium, the absorbance measured for a given amount of absorber in the sample gets enhanced. Such absorbance enhancement effect is shown in Figure 1b) where the optical spectrum obtained for 120  $\mu$ M (3 nmol) of bromocresol green (BCG) loaded into a glass fiber membrane insert (1 mm thickness) results greater than the one corresponding to the same amount of BCG in aqueous solution. The signal baseline registered for the membrane (no BCG) was also increased as a consequence of the multiscattering (light loss) and therefore in Figure 1b) the background was corrected to improve the readability of the graph. In order to further characterize the behavior of this absorbance enhancement another experiment was conducted in which BCG was prepared in aqueous solutions exhibiting different values of *RI*. The addition of increasing amount of sucrose in water (0, 20, 40, 60 and 80 %) gave rise to BCG solutions with the corresponding *RI* values of: 1.333, 1.364, 1.400, 1.442 and 1.490. Considering

the  $RI$  value of the glass fiber membrane (borosilicate),  $RI_{\text{membrane}} \approx 1.54$ , it is interesting to notice that the absorbance peak value corresponding to BCG (621 nm) decreases almost linearly when  $RI_{\text{medium}}$  is getting closer to  $RI_{\text{membrane}}$ . Furthermore, the interpolation of the linear dependency to the point at which  $RI_{\text{membrane}} \approx RI_{\text{medium}}$  ( $\Delta RI \approx 0$ ) gives a peak height value close to the one obtained for BCG in water and in absence of membrane. At this particular point the membrane becomes transparent and the membrane/medium system can now be defined as a uniform medium where propagating light is no longer getting scattered. The enhancement factor (EF) is 1 at  $\Delta RI = 0$  and then progressively increases with  $\Delta RI$  (i.e. when  $RI$  medium becomes lower) until it reaches a maximum value of almost  $EF = 30$  when the membrane initially loaded with BCG in water is left to dry for 48 hours ( $\Delta RI_{\text{max}}$ ). In the case of medium = air the absorbance response is higher than what should be expected from the extrapolation of the dependency obtained for water/sucrose system. This can be due to some changes taking place in the geometrical characteristics of the membrane during the drying process (e.g. pore size, thickness) and which affect the modification of the light path length. However, for a given membrane geometry the observed dependency of the absorbance enhancement on the heterogeneity of the system in terms of  $\Delta RI$  at the membrane/medium interfaces clearly confirms that the elongation of the light path length generated under a multiple scattering regime is responsible for the observed enhancement phenomenon.



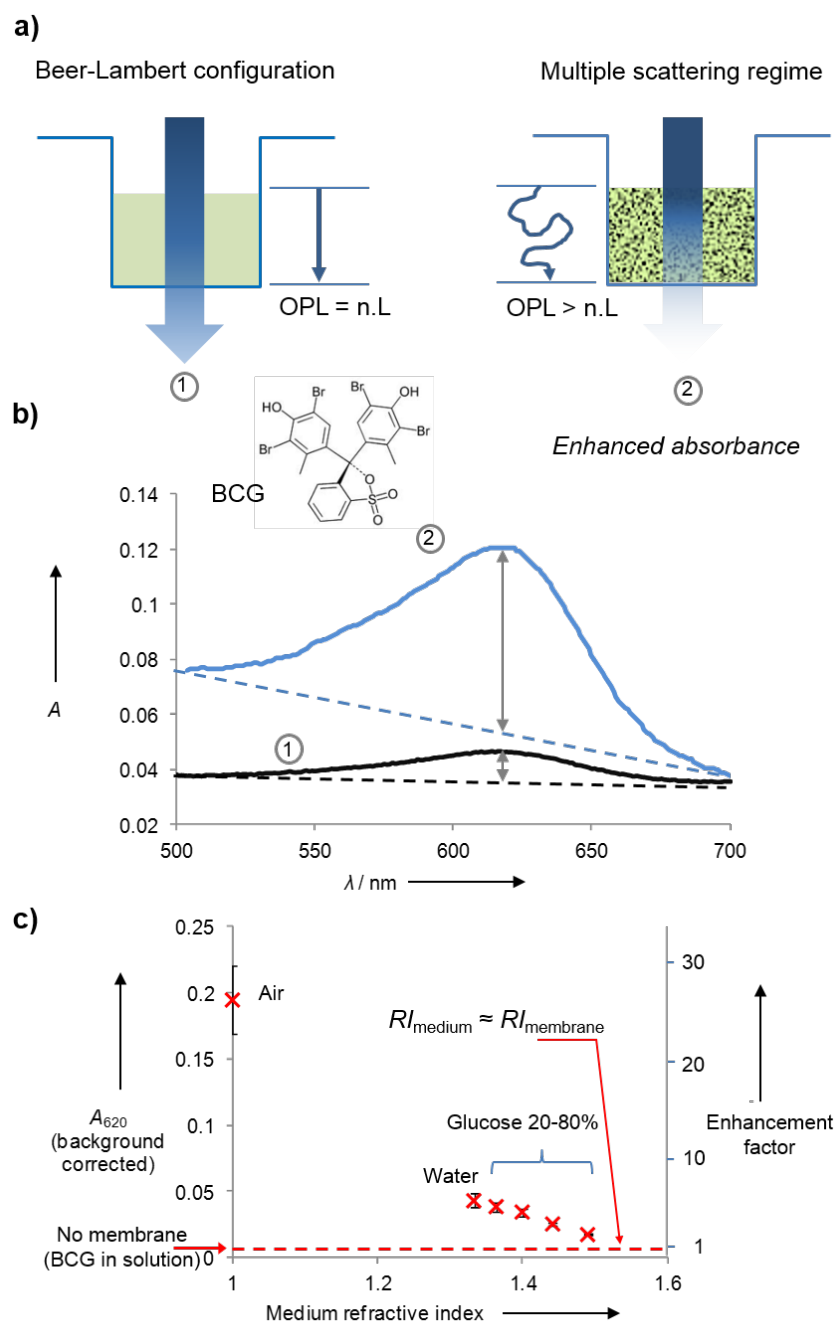


**Figure 1. a)** Detection principle based on the enhancement of the absorbance for a given molecule loaded in a random medium due to the elongation of the optical path length under multiple scattering regime. In comparison to the standard Beer-Lambert configuration where the absorbance measurements are performed in solution (1), a significant enhancement is observed when the molecule is loaded into a strongly scattering medium (2). **b)** Experimentally, the absorbance spectra of bromocresol green (3 nmol BCG) were measured in aqueous solution (1) and loaded into a glass fibre membrane (2). The height of BCG absorption peak (621 nm) was calculated (baseline between 500-700 nm) for varying values of  $\Delta RI = RI_{\text{membrane}} - RI_{\text{medium}}$ . **c)** The corresponding plot clearly indicates that the absorbance enhancement factor increases with  $\Delta RI$  (maximum enhancement for membrane/air configuration). Ideally, there is no absorbance enhancement (EF = 1) when  $RI_{\text{medium}}$  is close to the value corresponding to the membrane material (i.e. borosilicate  $RI=1.54$ ).

On the basis of this absorbance enhancement principle, and as a proof of concept, a versatile

detection system was established which enabled the development of two H<sub>2</sub>O<sub>2</sub> biosensors with improved sensitivity in a 96-wells microplate format. As depicted in Figure 2, enhancer inserts made from glass fiber membrane are biofunctionalized with the recognition biomolecule of interest – here an H<sub>2</sub>O<sub>2</sub> sensitive enzyme – in the presence of a chemical crosslinker (0.5% glutaraldehyde). The bio-active enhancer inserts are introduced into clean wells on the bottom of which circular apertures have priority been drilled in the centre (1.5 mm diameter). The detection protocol consists of adding 100 µL of sample mixture into each well modified with insert and left for 5 minutes. Then, a vertical flow is generated by putting the microplate in contact to an absorbent pad (driven by capillary forces) forcing the whole sample volume to get through the analyte-sensitive insert. Finally, absorbance measurements are performed on each individual well using a standard microplate reader. Noticeably, the term biosensor is voluntarily used here as it refers to a detection system where the recognition biomolecule (H<sub>2</sub>O<sub>2</sub> sensitive protein) is immobilized on the transducer surface (membrane glass fibers), in contrast to bioassay in which all the (bio)reagents stand in solution (Renneberg et al. 2008).

The first biosensor configuration described in Figure 3 relies on measuring the oxidation of cytochrome *c*, a globular hemoprotein (12.4 kDa), that occurs in the presence of H<sub>2</sub>O<sub>2</sub>. This ability of H<sub>2</sub>O<sub>2</sub> to oxidize ferrocyanochrome *c* have been first shown by Vandewalle et al. as the basis for an absorbance assay in which the decrease of ferrocyanochrome *c* peak at 550 nm was directly related to the concentration of H<sub>2</sub>O<sub>2</sub> in the cuvette (Vandewalle and Petersen 1987). Therefore, in our study glass fiber inserts were modified with reduced cytochrome *c* (0.62 nmol) and the decrease in the peak height (550 nm) consecutive to sample processing was calculated considering the baseline between 542 and 556 nm (intersection points for reduced and oxidized cytochrome *c* spectra). Similar absorbance value calculations were performed in control

experiment where the same amount of reduced cytochrome *c* (25  $\mu$ L of 25  $\mu$ M solution) was added into PBS-containing standard wells in the absence of any absorbance enhancer insert. The corresponding sigmoidal dose-response curves shown in Figure 3c) were analysed using the four-

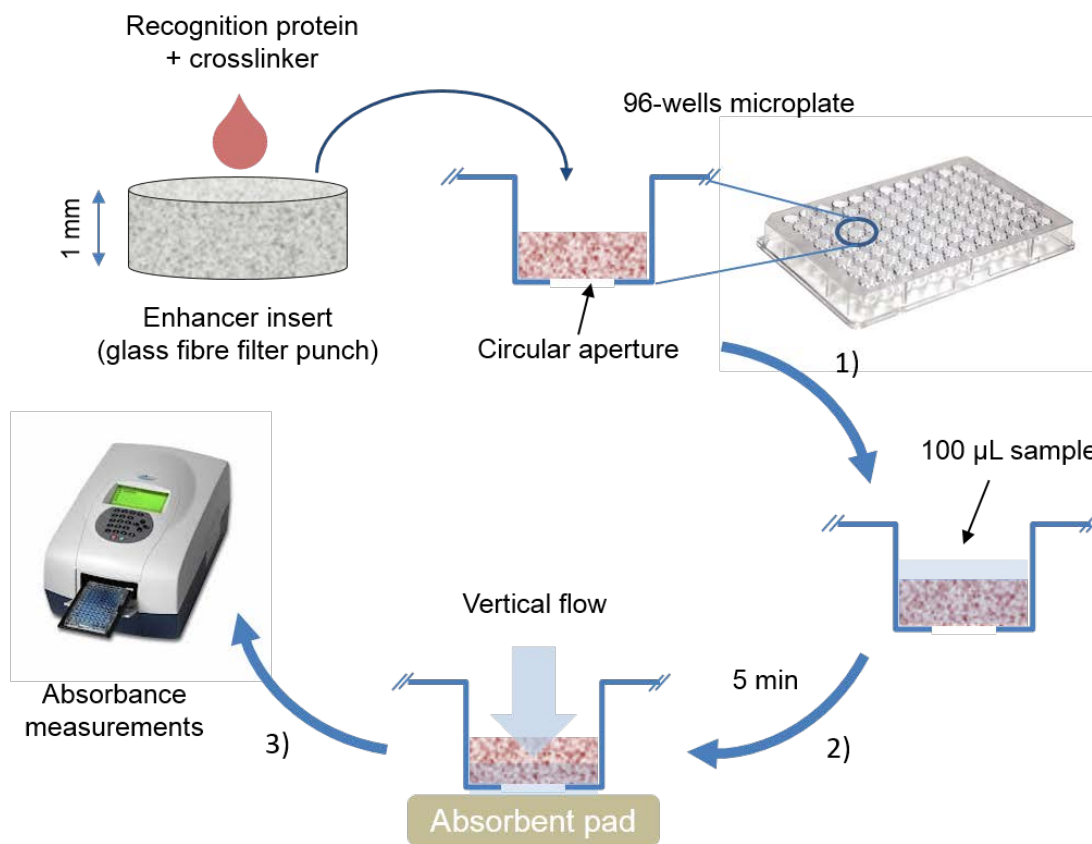


**Figure 2.** Schematic description of experimental setup. Glass fibre punch (filtration membrane) is loaded with the recognition protein in the presence of glutaraldehyde (0.5%). The biofunctionalized filter punch is used as absorbance enhancer insert and placed at the bottom of a microplate well. Priorly, circular apertures were drilled on the bottom of the wells in order to improve sample mass transport using capillary forces. The detection protocol consists of introducing 100  $\mu$ L of sample in the sensing well (1), which is then let to flow through the insert after 5 min (2). Changes in absorbance are measured using a standard microplate reader spectrometer (3).

parameter log-logistic (4-PL) fitting approach and the calculated parameters are summarized in the Table S1 of Supplementary Content (Findlay and Dillard 2007). Evidently, a significant absorbance gain is visible in the case of cytochrome *c* oxidation takes place in the enhancer inserts, as reflected by the corresponding signal amplitude value (top-bottom) being more than 6-fold greater than for the membrane-less bioassay. The limit-of-detection was calculated (response

at 3-folds the standard deviation for blank) for both configurations with and without the enhancer inserts and found to be: 3 and 147  $\mu\text{M}$ , respectively. This significant improvement of the limit-of-detection was obtained in spite of the increase of the standard deviation values calculated for the membrane insert-based biosensor. In order to evaluate comparatively the sensitivity of the two detection approaches, the sensitivity  $S_{50}$  at the inflection point of the curve defined as the ratio between the half-maximum absorbance and the corresponding  $\text{H}_2\text{O}_2$  concentration,  $C_{50}$ , were assessed. In comparison to the membrane-less bioassay configuration the calculated  $S_{50}$  values report a sensitivity enhancement of more than 40-folds in the case of the membrane insert biosensor. In other words, the analysis of the dose-response curves provides a clear indication that the developed biosensor approach improves significantly the analytical performances of the detection assay. The overall analytical improvement of the detection assay has to be attributed not only to the optical enhancement due to the elongation of the light path length but also to the efficient mass transport enabled by the vertical flow generated through the  $\text{H}_2\text{O}_2$ -sensitive enhancer insert. With this practical procedure the whole sample volume is forced to flow through the membrane and thus no limitation associated to low diffusion rate is observed. Consequently, the response time for the enhanced assay resulted shorter in comparison to the assay in solution, dropping down from 30 to 5 minutes. As a general comment, this aspect strongly emphasizes the adaptability of biosensors versus bioassays due to the fact that the recognition biomolecule is retained on the solid phase transducer and therefore larger volumes of sample can be eluded with no dilution issue. Besides, the versatility of the detection enhancement approach was explored in another biosensor configuration that involved the HRP enzymatic activity. HRP is a hemoprotein (40 kDa) frequently used as a label protein in ELISA tests since it catalyzes the oxidation of a series of chromogenic or fluorescent compounds in the presence of  $\text{H}_2\text{O}_2$ .

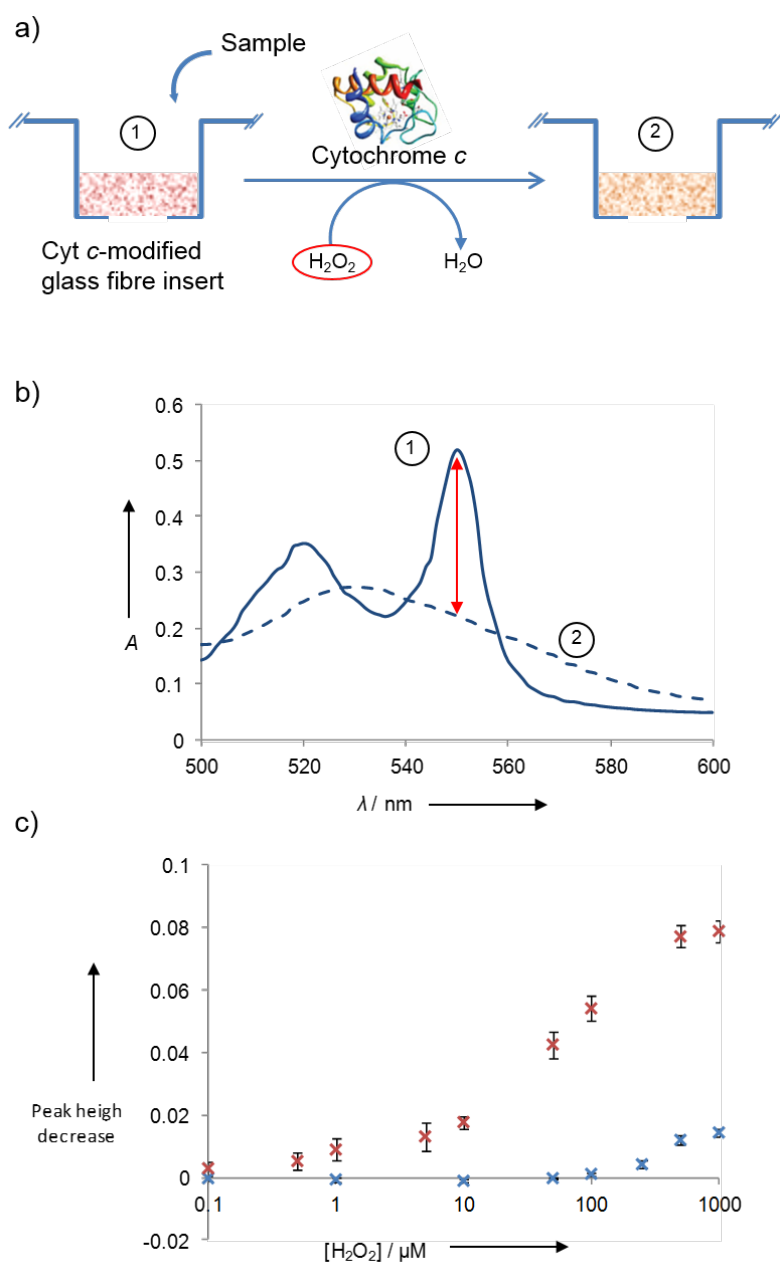


**Figure 3.** **a)** Biosensor configuration for  $H_2O_2$  detection based on the enhanced absorbance measurement of cytochrome *c* oxidation. Clean glass fibre inserts are modified with reduced cyt *c* and washed several times prior to experiments. **b)** Cytochrome *c* oxidation in the presence of  $H_2O_2$  induces a decrease in the absorption peak at 550 nm (baseline between 542 and 556 nm). **c)** Calibration curves obtained with 0.62 nmol (25 $\mu$ L of 25  $\mu$ M solution) of reduced cytochrome *c* either (blue) directly in PBS buffer solution (no insert) or (red) crosslinked into a glass fiber enhancer insert, and exposed to varying concentrations of  $H_2O_2$  (0.5  $\mu$ M to 1 mM contained in 100 $\mu$ L sample). The corresponding graph clearly shows the gain in sensitivity and limit of detection obtained when enhancer inserts are placed into the wells. Response times were 30 and 5 minutes for solution bioassay and insert-based biosensor, respectively. Error bars indicate the calculated standard deviation ( $n=3$ ).

In contrast to the biosensing approach previously described which relies on the detection of

spectral changes affecting the immobilized protein, i.e. cytochrome *c* oxidation, the detection principle now consists of measuring the development of a product enzymatically catalyzed. For the latter strategy it is required that the enzymatic product exhibits a poor solubility in water and forms a coloured precipitate which remains inside the glass fiber membrane insert, that is where optical path enhancement occurs. In that context, it appeared appropriate to choose AEC, a commonly used chromogen for staining peroxidases in tissue and cell preparations or even for characterizing catalytic activity of immobilized HRP monolayers (Suárez et al. 2007). As depicted in Figures 4A and 4B, for this second biosensor configuration the membrane inserts were biofunctionalized with HRP (0.62 nmol) and the progressive development of reddish precipitate in the presence of H<sub>2</sub>O<sub>2</sub> and AEC was measured as an absorbance increase at 580 nm. Similarly as before, control experiments were performed with the same amount of HRP in solution (25 µL of 1 mg.mL<sup>-1</sup>) in order to evaluate the analytical gain generated in the biosensor approach. The analysis of the corresponding dose-response curves via the 4-PL model equation reveals that the maximum absorbance value obtained in the membrane insert configuration is more than 3-folds higher than for the bioassay in solution. However, the calculated limits-of-detection were found to be in the same order of magnitude, 1 and 3 µM for the bioassay in solution and the membrane insert biosensor, respectively. In terms of sensitivity, the calculated values for S<sub>50</sub>, as earlier defined, indicate an enhancement in sensitivity of 7-folds in the case of the membrane insert approach. Moreover, the benefit in generating an active mass transport through the sensitive insert was manifest in the decrease of response time from 15 to 5 minutes. Even though the analytical gain arises clearly from this comparative study it is noticeable that a more dramatic contrast was evidenced with the earlier biosensor scheme based on cytochrome *c* oxidation. One possible explanation is that some AEC product generated in the membrane insert might have been washed away during sample elution. This signal loss is unlikely to occur in the

cytochrome *c*-based biosensor since the protein is covalently attached to the solid phase insert.

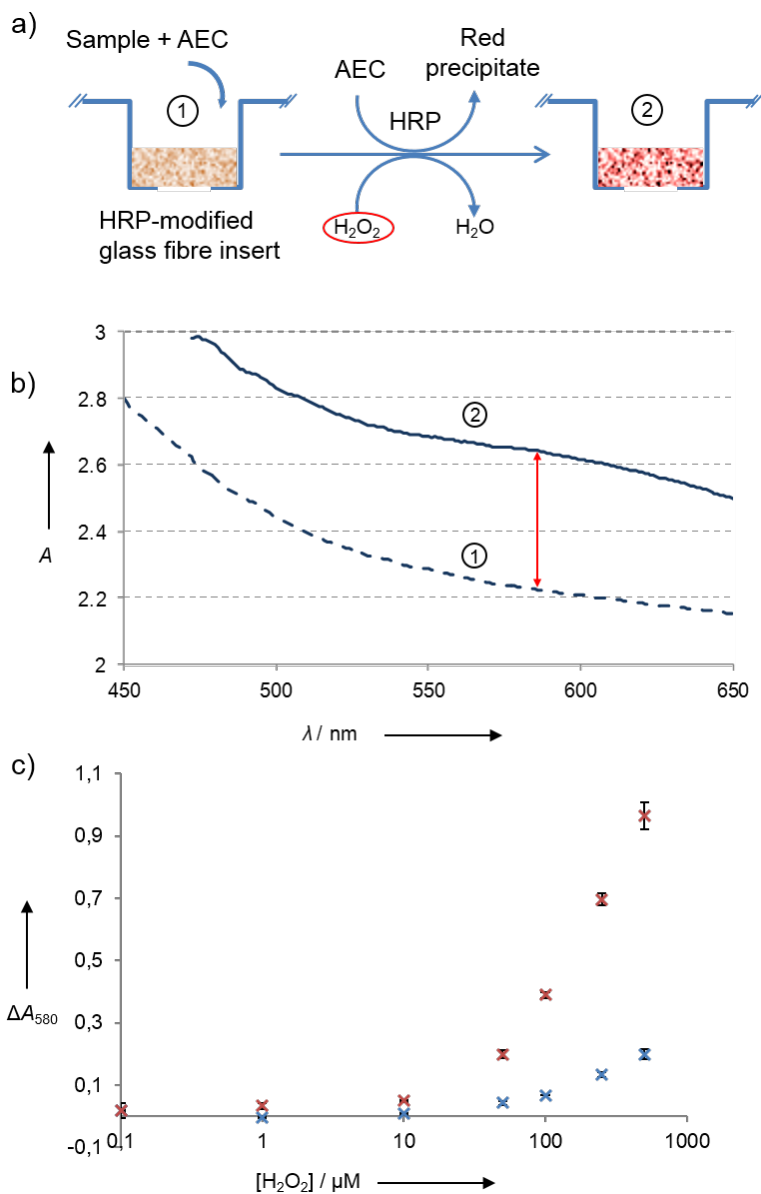


**Figure 4.** a) Biosensor configuration for  $H_2O_2$  detection based on the enhanced absorbance measurement of the catalytic conversion of HRP co-substrate, AEC, into an insoluble reddish product. Clean glass fibre inserts are modified with HRP and washed several times prior to experiments. b) The production of red precipitate in the presence of  $H_2O_2$  induces an increase in the measured absorbance ( $A_{max} = 580$  nm). c) Calibration curves were performed using 0.6 nmol of HRP (25  $\mu L$  of 1  $mg \cdot mL^{-1}$  solution) either (blue) directly in acetate buffer solution (no insert) or (red) crosslinked into a glass fibre enhancer insert, and exposed to varying concentrations of  $H_2O_2$  (1 to 500  $\mu M$  contained in 100  $\mu L$  sample) in the presence of AEC (142 nmol). The graphs indicate a significant improvement of the biosensor analytical performances in the case of HRP-modified enhancer insert. Response times: 15 and 5 minutes for solution assay and insert-based biosensor, respectively. Error bars indicate the calculated standard deviation ( $n=3$ ).

## CONCLUSION

In conclusion, the possibility to employ the absorbance enhancement phenomenon as a novel transduction principle suitable for microplate format assays has been successfully demonstrated. Inserts made of glass fiber membrane generate a significant absorbance gain which is dependent on the refractive index difference between the membrane and the surrounding medium. Therefore, the biofunctionalisation of membrane inserts with H<sub>2</sub>O<sub>2</sub>-sensitive proteins gave rise to the development of biosensors exhibiting improved analytical performances. Particularly in the case of cytochrome *c*-based biosensor the measured sensitivity was 40-folds greater than for the corresponding bioassay in solution while the limit-of-detection dropped down by a factor of 50-folds. In addition to their optical enhancement properties the membrane inserts act as a solid phase through which the whole sample volume can easily be eluded resulting in shorter response time while contributing to the overall improvement of the analytical gain. Finally, this simple biosensor strategy based on both absorbance enhancement and solid-phase configuration enabled by the use of glass fiber inserts, appears to be particularly appropriate to improve the analytical performances of existing bioassays via their effective conversion into highly sensitive biosensors.

## ACKNOWLEDGMENT

This work was supported by the Swiss National Science Foundation (projects 406440\_131282 and 406440\_131280 in the framework of the Swiss National Research Program NRP 64)

### **Supplementary content:**

- Calibration curves analysis via 4-parameter log-logistic (4-PL) treatment

## REFERENCES



- Chen, C., Song, G.T., Ren, J.S., Qu, X.G., 2008. A simple and sensitive colorimetric pH meter based on DNA conformational switch and gold nanoparticle aggregation. *Chem. Commun.*(46), 6149-6151.
- Ding, N., Yan, N., Ren, C., Chen, X., 2010. Colorimetric Determination of Melamine in Dairy Products by Fe(3)O(4) Magnetic Nanoparticles-H(2)O(2)-ABTS Detection System. *Anal. Chem.* 82(13), 5897-5899.
- Findlay, J.W.A., Dillard, R.F., 2007. Appropriate calibration curve fitting in ligand binding assays. *Aaps J.* 9(2), E260-E267.
- Gao, L.Z., Zhuang, J., Nie, L., Zhang, J.B., Zhang, Y., Gu, N., Wang, T.H., Feng, J., Yang, D.L., Perrett, S., Yan, X., 2007. Intrinsic peroxidase-like activity of ferromagnetic nanoparticles. *Nat. Nanotechnol.* 2(9), 577-583.
- Gillespie, K.M., Ainsworth, E.A., 2007. Measurement of reduced, oxidized and total ascorbate content in plants. *Nat. Protoc.* 2(4), 871-874.
- Grumann, M., Steigert, J., Riegger, L., Moser, I., Enderle, B., Riebeseel, K., Urban, G., Zengerle, R., Ducree, J., 2006. Sensitivity enhancement for colorimetric glucose assays on whole blood by on-chip beam-guidance. *Biomed. Microdevices* 8(3), 209-214.
- John, S., Pang, G., 1996. Theory of lasing in a multiple-scattering medium. *Phys. Rev. A* 54(4), 3642-3652.
- Kuang, Y., Salem, N., Wang, F.J., Schomisch, S.J., Chandramouli, V., Lee, Z.H., 2007. A colorimetric assay method to measure acetyl-CoA synthetase activity: Application to woodchuck model of hepatitis virus-induced hepatocellular carcinoma. *J. Biochem. Biophys. Methods* 70(4), 649-655.
- Liu, J.W., Lu, Y., 2003. A colorimetric lead biosensor using DNAzyme-directed assembly of gold nanoparticles. *J. Am. Chem. Soc.* 125(22), 6642-6643.
- Liu, J.W., Mazumdar, D., Lu, Y., 2006. A simple and sensitive "dipstick" test in serum based on lateral flow separation of aptamer-linked nanostructures". *Angew. Chem.-Int. Edit.* 45(47), 7955-7959.
- Malcik, N., Ferrance, J.P., Landers, J.P., Caglar, P., 2005. The performance of a microchip-based fiber optic detection technique for the determination of Ca(2+) ions in urine. *Sens. Actuator B-Chem.* 107(1), 24-31.
- Mao, X., Ma, Y.Q., Zhang, A.G., Zhang, L.R., Zeng, L.W., Liu, G.D., 2009. Disposable Nucleic Acid Biosensors Based on Gold Nanoparticle Probes and Lateral Flow Strip. *Anal. Chem.* 81(4), 1660-1668.
- Martinez, A.W., 2011. Microfluidic paper-based analytical devices: from POCKET to paper-based ELISA. *Bioanalysis* 3(23), 2589-2592.
- Plested, J.S., Coull, P.A., Gidney, M.A.J., 2003. ELISA. *Methods in molecular medicine* 71, 243-261.

Popescu, G., Dogariu, A., 1999. Optical path-length spectroscopy of wave propagation in random media. *Opt. Lett.* 24(7), 442-444.

Renneberg, R., Pfeiffer, D., Lisdat, F., Wilson, G., Wollenberger, U., Ligler, F., Turner, A.P.F., 2008. Frieder scheller and the short history of biosensors. In: Renneberg, R., Lisdat, F. (Eds.), *Biosensing for the 21st Century*, pp. 1-18. Springer-Verlag Berlin, Berlin.

Sato, K., Hosokawa, K., Maeda, M., 2003. Rapid aggregation of gold nanoparticles induced by non-cross-linking DNA hybridization. *J. Am. Chem. Soc.* 125(27), 8102-8103.

Song, Y., Wei, W., Qu, X., 2011. Colorimetric Biosensing Using Smart Materials. *Advanced Materials* 23(37), 4215-4236.

Suárez, G., Jackson, R.J., Spoons, J.A., McNeil, C.J., 2007. Chemical introduction of disulfide groups on glycoproteins: A direct protein anchoring scenario. *Anal. Chem.* 79(5), 1961-1969.

Suárez, G., Santschi, C., Dutta-Gupta, S., Juillerat-Jeanneret, L., Martin, O.J.F., 2012. Biophotonic Sensor for Real-time and Non-invasive Detection of Extracellular H<sub>2</sub>O<sub>2</sub> Released by Stimulated Cells. *Procedia Engineering* 47(0), 1281-1283.

Suárez, G., Santschi, C., Slaveykova, V.I., Martin, O.J.F., 2013. Sensing the dynamics of oxidative stress using enhanced absorption in protein-loaded random media. *Sci. Rep.* 3, 3447

Svensson, T., Shen, Z.J., 2010. Laser spectroscopy of gas confined in nanoporous materials. *Appl. Phys. Lett.* 96(2).

Vandewalle, P.L., Petersen, N.O., 1987. OXIDATION OF REDUCED CYTOCHROME-C BY HYDROGEN-PEROXIDE - IMPLICATIONS FOR SUPEROXIDE ASSAYS. *Febs Letters* 210(2), 195-198.

Zhang, J.Z., 2006. Enhanced sensitivity in flow injection analysis using a long pathlength liquid waveguide capillary flow cell for spectrophotometric detection. *Anal. Sci.* 22(1), 57-60.

# Supplementary Content

## Calibration curve 4-PL analysis

The calibration curves were analyzed through the 4-parameters log-logistic fit:

$$A = a + \frac{b-a}{1 + \left(\frac{c}{c_{50}}\right)^{Hillslope}}$$

**Table S1.** Analytical parameters obtained for the insert-based biosensors and corresponding bioassay in solution for both detection systems based on cytochrome *c* and HRP/AEC.

	Cytochrome <i>c</i>		HRP/AEC	
	Bioassay (solution)	Biosensor (insert)	Bioassay (solution)	Biosensor (insert)
<i>a</i>	0.015	0.087	0.380	1.390
<i>b</i>	0.0002	0.0037	0.004	0.020
<i>C</i> <sub>50</sub> / μM H <sub>2</sub> O <sub>2</sub>	325	59	467	251
<i>Hillslope</i>	2.96	0.85	1.02	1.14
<i>LoD</i> / μM	147	3	1	3
<i>S</i> <sub>50</sub> / M <sup>-1</sup> H <sub>2</sub> O <sub>2</sub>	200	770	400	280